Cell

Caspase-1 Activation of Lipid Metabolic Pathways in Response to Bacterial Pore-Forming Toxins Promotes Cell Survival

Laure Gurcel,[1] Laurence Abrami,[1] Stephen Girardin,[3] Jurg Tschopp,[4] and F. Gisou van der Goot[1,2,5,*]
[1] Department Microbiology and Molecular Medicine, University of Geneva, 1 rue Michel Servet, CH-1211 Geneva 4, Switzerland
[2] Ecole Polytechnique de Lausanne, Global Health Institute, Station 15, CH-1015 Lausanne, Switzerland
[3] Institut Pasteur, 25 rue du Dr Roux, F-75724 Paris, France
[4] Department Biochemistry, University of Lausanne, Chemin des Boveresses 155, CH-1066 Epalinges, Switzerland
[5] Ecole Polytechnique de Lausanne, Institute of Global Health, Station 15,1015 Lausanne, Switzerland
*Contact: gisou.vandergoot@epfl.ch
DOI 10.1016/j.cell.2006.07.033

SUMMARY

Many pathogenic organisms produce pore-forming toxins as virulence factors. Target cells however mount a response to such membrane damage. Here we show that toxin-induced membrane permeabilization leads to a decrease in cytoplasmic potassium, which promotes the formation of a multiprotein oligomeric innate immune complex, called the inflammasome, and the activation of caspase-1. Further, we find that when rendered proteolytic in this context caspase-1 induces the activation of the central regulators of membrane biogenesis, the Sterol Regulatory Element Binding Proteins (SREBPs), which in turn promote cell survival upon toxin challenge possibly by facilitating membrane repair. This study highlights that, in addition to its well-established role in triggering inflammation via the processing of the precursor forms of interleukins, caspase-1 has a broader role, in particular linking the intracellular ion composition to lipid metabolic pathways, membrane biogenesis, and survival.

INTRODUCTION

Pathogenic micro-organisms, and in particular bacteria, often produce pore-forming proteins as virulence factors (van der Goot, 2001). These proteins are either bonafide pore-forming toxins or components of type III secretion apparatus involved in perforating the host plasma membranes to allow the injection of bacterial effectors necessary for infection (Mota et al., 2005). The size of the pores varies from 1–2 nm for pore-forming toxins such as aerolysin from *Aeromonas hydrophila* (Abrami et al., 2000) or α-toxin from *Staphylococcus aureus* (Bhakdi and Tranum-Jensen, 1991), to 25–30 nm for Cholesterol Dependent Toxin such as pneumolysin or listeriolysin O (Shatursky et al., 1999). Depending on the toxin, its concentration, and the type of target cell, the outcome of the toxin-induced plasma membrane perforation may also vary. The two extreme cases are osmotic lysis of erythrocytes, which are not necessarily physiological targets of these toxins, and full-membrane repair and cell survival (Walev et al., 2001; Walev et al., 1994). The most common outcome in vitro is however cell death—which can be apoptotic or necrotic but has generally not been characterized (Abrami et al., 2000). Little is known however about the underlying cellular mechanisms.

Here we were interested in cellular responses to pore-forming toxins, in particular survival mechanisms. We used aerolysin as a prototype since it is well characterized (Abrami et al., 2000), and a variety of inactive mutants are available (Fivaz et al., 2002; Tsitrin et al., 2002). The toxin is secreted by *Aeromonas* species as an inactive precursor, called proaerolysin, which must be proteolytically processed by gut enzymes or by proteases of the furin family (Abrami et al., 2000). The precursor, as well as the mature toxin, binds specifically to GPI-anchored proteins at the surface of target cells (Abrami et al., 2000). Once bound and processed, the toxin heptamerizes into a circular ring, a process that is promoted by lipid rafts (Abrami and van der Goot, 1999). Toxin oligomerization leads to the exposure of hydrophobic surfaces that drive membrane insertion (Iacovache et al., 2006). Pore formation renders the plasma membrane permeable to small ions but not proteins (Abrami et al., 2000). Specific cellular effects observed upon aerolysin treatment are release of calcium from the endoplasmic reticulum (ER); vacuolation of the ER (Abrami et al., 2000); and production of proinflammatory molecules such as tumor necrosis factor α (TNFα), interleukin 1β, interleukin 6, and prostaglandin E2 (Chopra et al., 2000; Galindo et al., 2004a). We show here that, by allowing the efflux of intracellular potassium, aerolysin triggers the activation of caspase-1. This cysteine protease is produced as a 45 kDa precursor that requires autocatalytic processing for activation.

Autoproteolysis depends on the formation of a large multiprotein oligomeric complex called the inflammasome (Martinon and Tschopp, 2005), which brings procaspase-1 molecules in close proximity of one another. Two types of inflammasomes have been reported, each containing a different member of the intracellular pattern recognition receptors, the so-called NLR (NACHT-LRR) family of proteins (Martinon and Tschopp, 2005). NLR members are typically composed of three domains: a leucine rich repeat (LRR) ligand-sensing domain, a NACHT oligomerization domain, and a C-terminal homotypic protein-protein interaction domain that can be either a caspase recruitment domain (CARD) or a pyrin domain. Recently some natural stimuli of the inflammasomes have been identified, such as uric acid crystals associated with Gout (Martinon et al., 2006), bacterial RNA (Kanneganti et al., 2006), extracellular ATP, the calcium channel affecting marine toxin maitotoxin (Mariathasan et al., 2006) and cytoplasmic flagellin (Franchi et al., 2006; Miao et al., 2006), leading to the view that inflammasomes are intracellular detectors of danger signals. Two NLR members can induce caspase-1 activation: NALP and IPAF. Genomic analysis has revealed 14 NALPs in the human genome, of which NALP1 and NALP3 have been best characterized and shown to be involved in caspase-1 activation (Chamaillard et al., 2003). The interaction of NALPs with caspase-1 is not direct and depends on the adaptor protein ASC (apoptosis-associated speck-like protein containing a CARD) (Martinon and Tschopp, 2005). IPAF, for which only one form has been reported, in contrast associates directly with caspase-1 via its C-terminal CARD domain (Martinon and Tschopp, 2005), although direct or indirect interactions with ASC may exist (Mariathasan et al., 2004; Sutterwala et al., 2006).

We here found that aerolysin-induced K^+ efflux triggers the assembly of IPAF and the NALP3 inflammasomes and the activation of caspase-1. Most importantly, we found that caspase-1 then induces the activation of the central regulators of membrane biogenesis, the sterol regulatory element binding proteins (SREBPs), which in turn promote cell survival upon toxin challenge. This study highlights that, in addition to its well-established role in triggering inflammation via the processing of the precursor forms of interleukins 1β, 18 (Fantuzzi and Dinarello, 1999), and 33 (Schmitz et al., 2005), caspase-1 has a broader role than previously appreciated, in particular linking the intracellular ion composition to lipid metabolic pathways.

RESULTS AND DISCUSSION

Pore Formation by Aerolysin Leads to the Activation of SREBPs

To study the cellular response to pore-forming toxins, we performed an RNA differential display analysis using the highly sensitive amplification of double-stranded cDNA end restriction (ADDER) fragments method (Kornmann et al., 2001). Chinese hamster ovary (CHO) cells were treated with low concentrations of proaerolysin (0.1 nM [Ratner et al., 2006]), conditions under which all cells excluded the DNA-intercalating agent propidium iodide for at least 10 hr (Figure S1A) (note that the protoxin is processed to aerolysin by cell-surface proteases, leading to pore formation). The ADDER analysis led to the identification of various differentially expressed genes, in particular the sterol regulatory element binding protein-2 (SREBP-2), which was upregulated after 3 hr (Figure S1B). SREBPs are membrane bound transcription factors that regulate the expression of genes harboring a sterol responsive element (SRE) in their promoter region and which are typically involved in cholesterol and fatty acid biosynthesis (for review see Goldstein et al., 2006). SREBPs initially reside in the ER. Release of the transcription factor domain from the membrane requires sequential proteolysis by two transmembrane enzymes, S1P and S2P, which reside in the Golgi apparatus. Cleavage of SREBPs thus requires transport from the ER to the Golgi, a step that is controlled by the escort protein SCAP (Goldstein et al., 2006). The following three major SREBP isoforms are known: SREBP-1a and -1c, which are encoded by a single gene and are preferentially involved in fatty acid metabolism, and SREBP-2, which is encoded by a distinct gene and controls cholesterol and lipid biosynthesis (Goldstein et al., 2006; Horton and Shimomura, 1999). Different stimuli have been reported to induced SREBP activation, including cholesterol depletion (Goldstein et al., 2006), ER calcium depletion (Lee and Ye, 2004), growth factors and insulin signaling (Demoulin et al., 2004; Nadeau et al., 2004), phagocytosis (Castoreno et al., 2005), and exposure of cells to hypotonic media (Lee and Ye, 2004).

Since regulation of SREBPs mainly occurs at the protein level rather than the transcriptional level, we tested whether aerolysin triggers SREBP-2 processing. Membrane and nuclear fractions were prepared from toxin-treated cells and probed by Western blotting using an antibody against the N terminus of SREBP-2. In untreated cells, full-length SREBP-2 (123 kDa) was found in the membrane fraction (Figure 1A), as expected since cells were grown in the presence of serum, the high-lipid content of which suppresses SREBP activation. Upon aerolysin treatment, the amount of full-length SREBP-2 decreased with time with the concomitant appearance of an ~60 kDa form in the nuclear fraction. Migration of SREBP-2 to the nucleus was confirmed by immunofluorescence microscopy (Figure 1B). Interestingly, the second SREBP isoform, SREBP-1, also underwent activation upon toxin treatment (Figure 1C). These results show that aerolysin caused the proteolytic processing and nuclear translocation of SREBPs.

We next measured the effect of aerolysin on the mRNA levels of two SREBP target genes: HMGCoA reductase and fatty acid synthase activated by SREBP-2 and SREBP-1 respectively (Horton and Shimomura, 1999). Both mRNAs increased upon toxin addition as shown by real-time PCR (Figures 1D and 1E, >3 fold after 3 hr). Also, the total cellular cholesterol increased by 25% to 30% after 3–5 hr toxin treatment (Figure 1F). Similar

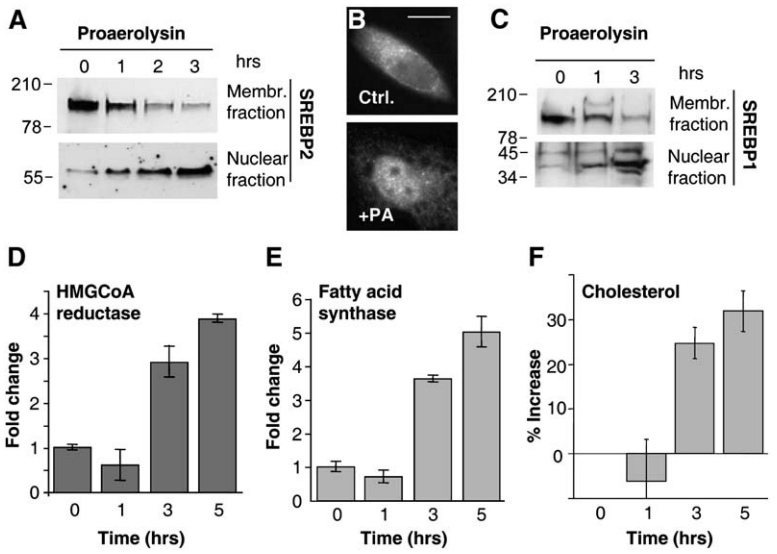

Figure 1. Aerolysin Triggers the Activation of SREBPs

(A) CHO cells were treated or not for 1, 2, or 3 hr with 0.2 nM proaerolysin. Membrane and nuclear fractions were prepared and probed for the presence of SREBP-2.

(B) Immunofluorescence against SREBP-2 of CHO cells treated or not with 0.2 nM aerolysin for 3 hr. Bar is 10 μm.

(C)–(E) CHO cells were treated as in (A), and cellular fractions were probed for SREBP-1. In (D) and (E), RNA was extracted from CHO cells treated or not with 0.2 nM proaerolysin for 1, 3, or 5 hr. Levels of HMGCoA reductase (D) and fatty acid synthase (E) mRNAs were quantified and normalized to the levels of mRNAs of translation elongation factor 1 α1 and transcription factor TATA Binding Protein, which did not significantly change upon toxin treatment. Error bars represent standard deviations (n = 3).

(F) CHO cells were treated as in (A), and the cellular cholesterol levels were determined and normalized to protein concentration. Error bars represent standard deviations (n = 3).

increases were observed whether cells were incubated in serum-free medium or in serum-containing medium, in the presence or absence of the cholesterol synthesis inhibitor lovastatin (not shown), indicating that cholesterol could be synthesized as well as taken up from the medium, in agreement with the regulatory effect of SREBP-2 on transcription of the LDL receptor gene.

Altogether, these observations show that aerolysin triggers the activation of SREBPs, the subsequent upregulation of genes under the control of SREs, and the increase of cellular cholesterol.

Toxin-Induced K^+ Efflux Triggers SREBP-2 Activation

To understand the mechanisms that mediate aerolysin-induced SREBP activation, we first investigated whether pore formation was required by using two inactive aerolysin mutants: ASSP, which binds to GPI-anchored proteins but is unable to form heptamers (Fivaz et al., 2002), and Y221G, which binds to GPI-anchored proteins and forms heptamers but is unable to insert into membranes (Tsitrin et al., 2002). Neither mutant affected SREBP-2, indicating that pore formation is necessary for activation of the transcription factor (Figure 2A). Since the same purification procedure was used for wild-type (WT) and mutant toxins, these observations also indicate that aerolysin-induced SREBP activation is not due to contaminating bacterial products, and in particular, lipopolysaccharide (LPS). This was confirmed by the lack of effect of LPS binding antibiotic polymixin B on aerolysin-induced SREBP-2 activation (Figure S2A). Pore formation per se thus appeared to be required for SREBP-2 activation. We thus wondered whether another pore-forming toxin would trigger the same lipogenic response, and α-toxin form *Staphylococcus aureus* was chosen since its mode of action and pore size are very similar to that of aerolysin (Bhakdi and Tranum-Jensen, 1991). In HeLa cells (CHO cells are insensitive to α-toxin), both aerolysin (see Figure 3A) and Staphylococcal α-toxin induced SREBP-2 activation (Figure 2B).

Since SREBP-2 is an ER membrane protein and we have previously shown that aerolysin triggers fragmentation and vacuolation of the ER (Abrami et al., 1998), we investigated whether SREBP-2 activation was due to toxin-induced ER alterations. Vacuolation can be prevented either by the addition of sucrose to the medium (unpublished data) or by chelating extracellular calcium (Abrami et al., 1998). Neither extracellular sucrose (Figure S2B) nor EGTA (Figure S2C) prevented SREBP-2 activation. These experiments also indicate that SREBP-2 activation is not due to calcium entry. A role of elevated intracellular calcium was further ruled out by the use of the intracellular calcium chelator BAPTA-AM, which had no effect on SREBP-2 activation (data not shown).

We then tested whether exit of potassium, through the toxin pores, could be the trigger for SREBP-2 activation. Cells were treated with aerolysin in a high (150 mM KCl) or low (5 mM KCl) K^+-containing medium or in tissue-culture medium (containing serum). No K^+ efflux was observed upon toxin treatment in high K^+ medium (data not shown), as expected, but, remarkably, SREBP-2 was not activated (Figure 2C), suggesting that K^+ efflux was necessary. To test whether K^+ efflux was sufficient, cells were treated with the K^+ ionophore valinomycin, and SREBP-2 activation was readily observed (Figure 2D). In contrast, monensin, a sodium ionophore (which was active under our experimental conditions, Figure S3), had no effect (data not shown), suggesting that SREBP-2 activation is due to K^+ efflux and not membrane depolarization.

It has previously been reported that thapsigargin-induced ER calcium release leads to SREBP activation (Lee and Ye, 2004). Although aerolysin also leads to ER calcium release (Krause et al., 1998), this event is not

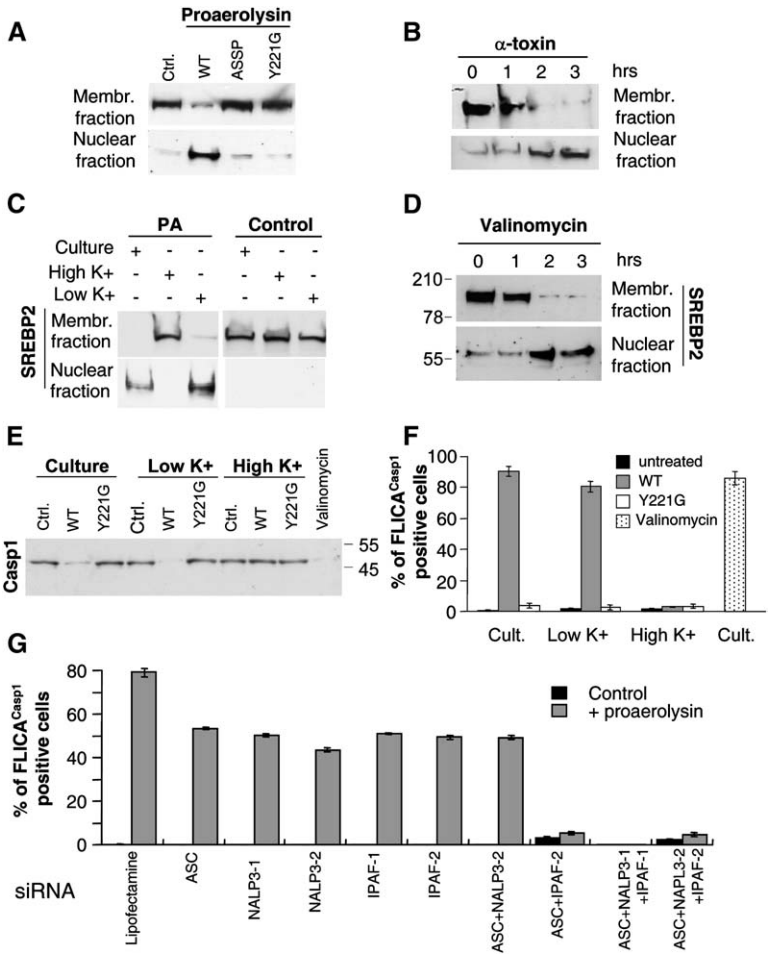

Figure 2. Aerolysin-Induced K^+ Efflux Triggers both SREBP-2 Maturation and Inflammasome-Mediated Caspase-1 Activation

(A) CHO cells were treated or not with 0.2 nM WT or ASSP and Y221G proaerolysins for 3 hr. Membrane and nuclear fractions were probed for the presence of SREBP-2.

(B) HeLa cells were treated for different times with Staphylococcal α-toxin (30 nM). Membrane and nuclear fractions were probed for SREBP-2.

(C) CHO cells, in tissue-culture medium (Culture), Hanks buffer (low K^+), or a modified Hanks buffer in which the sodium and K^+ concentrations were inverted (High K^+), were treated or not with 0.2 nM proaerolysin for 3 hr. Cellular fractions were analyzed as in (A).

(D) CHO cells were treated for different times with 10 μM of valinomycin. Cellular fractions were analyzed as in (A).

(E and F) CHO cells were treated or not with 0.2 nM WT or Y221G proaerolysin or 10 μM of valinomycin for 3 hr in either tissue-culture medium (Culture, Cult.), Hanks buffer (low K^+), or High K^+ as in (C). Activation of caspase-1 was monitored (E) by Western blotting to detect processing of the 45 kDa procaspase-1 or (F) using the fluorescent reagent, $FLICA^{Casp1}$. Error bars represent standard deviations (n = 3).

(G) HeLa cells were transiently transfected (24 hr) with RNAi duplexes against ASC, NALP3, and IPAF in single to triple transfections. Two duplex sequences, labeled 1 and 2, were used for NALP3 and IPAF. Cells were then treated with proaerolysin for 3 hr at 0.2 nM, and caspase-1 activation was monitored using $FLICA^{Casp1}$. Under each RNAi condition, the number of $FLICA^{Casp1}$-positive cells in the absence of toxin was extremely low and thus not visible on a *y* axis ranging from 0% to 80%. Error bars represent standard deviations (n = 3).

necessary for K^+ efflux-mediated SREBP-2 activation since valinomycin, which efficiently triggers SREBP-2 activation, has no effect on ER calcium (data not shown).

Aerolysin Triggers Inflammasome-Mediated Activation of Caspase-1

The above experiments show that the event that is sensed upstream of SREBP activation is the loss of intracellular K^+. Potassium efflux, triggered by *Staphylococcal* α-toxin (Walev et al., 2000), K^+ ionophores (Mariathasan et al., 2006; Perregaux and Gabel, 1994), or activation of the P2X7 receptor by extracellular ATP (Kahlenberg and Dubyak, 2004; Mariathasan et al., 2006), has been shown to activate caspase-1. We therefore analyzed the effect of aerolysin on caspase-1. As shown in Figure 2E, WT, but not Y221G mutant, aerolysin led to the processing of procaspase-1. Caspase-1 cleavage was however only observed when extracellular K^+ was low (Figure 2E), indicating that K^+ efflux was necessary and indeed caspase-1 activation could also be triggered by valinomycin (Figure 2E). Identical observations were made when using the commercially available fluorescent reagent, $FLICA^{Casp1}$, that binds to the active form of caspase-1 with high affinity (Figure 2F). Importantly, caspase-1 activation was equally observed with polymixin B-treated WT aerolysin, ruling out a role of contaminating LPS (Figure S4A). Finally aerolysin specifically activated caspase-1, since caspase-3 was not activated as monitored by Western blotting (data not shown) or using the caspase-3 specific $FLICA^{Casp3}$ reagent (Figure S4B).

To investigate whether the inflammasomes are involved in sensing the aerolysin-induced K^+ efflux, we silenced expression of IPAF, NALP3, and/or ASC by siRNA. All duplex RNAis efficiently reduced the levels of the corresponding mRNAs (Figure S5A) as well as the expression of the corresponding FLAG-tagged proteins (Figure S5B). Interestingly, knock down of ASC, NALP3, or IPAF individually led to a 30%–50% decrease in the number of cells in which caspase-1 was activated in response to aerolysin (Figure 2G), whereas the transfection of four irrelevant

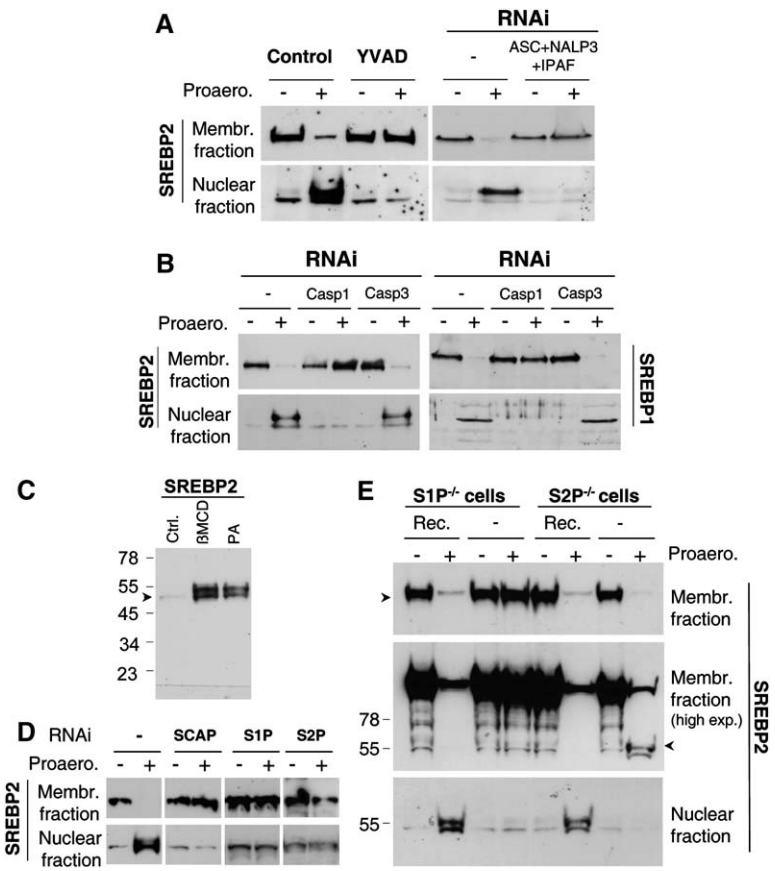

Figure 3. Aerolysin-Induced SREBP Activation Is Caspase-1 Dependent but S1P and S2P Mediated

(A) As shown in the left panel, CHO cells were treated or not with the caspase-1 inhibitor YVAD (100 μM) for 1 hr, followed by 3 hr with proaerolysin (0.2 nM), still in the presence or absence of inhibitor. Membrane and nuclear fractions were probed for the presence of SREBP-2. As shown in the right panel, HeLa cells were transiently transfected (24 hr) with RNAi duplexes against ASC, NALP3 (sequence 1), and IPAF (sequence 1), followed by 3 hr treatment with 0.2 nM proaerolysin. Membrane and nuclear fractions were prepared and analyzed (80 μg) for the presence of SREBP-2.

(B) HeLa cells were transiently transfected (24 hr) with RNAi duplexes against caspase-1 or -3, followed by 3 hr treatment with 0.2 nM proaerolysin. Membrane and nuclear fractions were probed for the presence of SREBP-2 (left panel) or SREBP-1 (right panel).

(C) CHO cells were treated either with β-methyl-cyclodextrin (βMCD, 10 mM) in a serum-free medium for 1 hr or with 0.2 nM proaerolysin for 3 hr. Nuclear fractions were probed for SREBP-2.

(D) HeLa cells were transiently transfected (48 hr) with RNAi duplexes against SCAP, S1P, or S2P, followed by 3 hr treatment with 0.2 nM proaerolysin. Membrane and nuclear fractions were probed for the presence of SREBP-2.

(E) S1P- or S2P-deficient CHO cells and the corresponding recomplemented CHO were treated with 0.2 nM proaerolysin for 3 hr. Membrane and nuclear fractions were probed for the presence of SREBP-2. Two different exposures of the membrane fraction are shown.

siRNAs had no effect (Figure S6A). Double transfection with siRNA against ASC and NALP3 did not lead to a further decrease, whereas knocking down ASC and IPAF together essentially abolished caspase-1 activation, as did triple transfection against all three components (Figure 2G). Again triple transfection using irrelevant siRNAs had no effect (Figure S6A). The inhibitory effect of these siRNAs were specific for inflammasome-mediated pathways since cotransfection of siRNAs against ASC and IPAF for example did not prevent activation of the interferon β pathway by Sendai virus (Strahle et al., 2006) (Figure 7).

These results show that aerolysin induces activation of caspase-1 through the assembly of both the IPAF and the NALP3 inflammasomes. It is interesting to note that toxin-induced K^+ efflux is to our knowledge the first stimulus that simultaneously activates both inflammasomes, raising the possibility that for such a severe stress, nature has conceived a backup pathway.

Aerolysin-Induced SREBP Activation Is Caspase-1 Mediated

Aerolysin-induced K^+ efflux triggers activation of both caspase-1 and SREBP-2. To determine whether these events lie in a common pathway, we investigated whether preventing one would affect the other. Remarkably, the caspase-1 inhibitor YVAD completely blocked aerolysin-induced SREBP-2 activation (Figure 3A, left panel), whereas the caspase-3 inhibitor DEVD had no effect (data not shown). Aerolysin-induced SREBP-2 activation could also be prevented by knocking down the inflammasomes using siRNAs against NALP3, ASC, and IPAF (Figure 3A, right panel) or by directly knocking down the expression of caspase-1 (Figure 3B, left panel). This effect was specific to caspase-1 since RNAi against caspase-3 had no effect (Figure 3B, left panel). RNAi against caspase-1, but not caspase-3, also prevented aerolysin-induced activation of SREBP-1 (Figure 3B, right panel). These observations show that caspase-1 activation lies upstream and is required for SREBP activation. In agreement with this sequence of events, preventing activation of SREBP-2 (see Experimental Procedures below) had no effect on aerolysin-induced caspase-1 activation (Figure S9B).

Caspase-1 Triggers S1P- and S2P-Mediated SREBP Activation

Since caspase-1 is a protease and since activation of SREBPs involves proteolysis, we investigated the possibility of a direct activation. Hamster SREBP-1 and -2

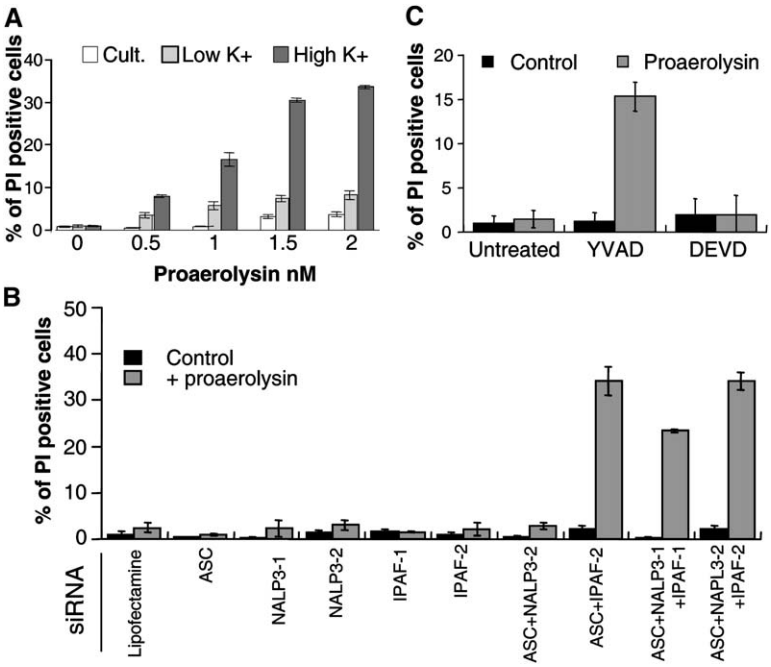

Figure 4. Preventing Caspase-1-Mediated SREBP-2 Maturation Promotes Aerolysin-Induced Cell Death

(A) CHO cells were incubated in tissue-culture medium (Culture) or Hanks buffer (low K^+) or a modified Hanks buffer, in which the sodium and potassium concentrations were inverted (High K^+). Cells were treated for 1 min with different concentrations of proaerolysin and then incubated in the corresponding medium for 4 hr prior to propidium iodide staining. Error bars represent standard deviations (n = 3).

(B) HeLa cells were transiently transfected (24 hr) with RNAi duplexes against ASC, NALP3, and IPAF in single to triple transfections. Two duplex sequences, labeled 1 and 2, were used for NALP3 and IPAF. Cells were then treated as in (A).

(C) CHO cells were treated or not with either the caspase-1 inhibitor YVAD (100 μM) or the caspase-3 inhibitor DEVD (100 μM) for 1 hr, followed by 3 hr with proaerolysin (0.2 nM), then stained with propidium iodide. Error bars represent standard deviations (n = 3).

each contain a potential caspase-1 cleavage site in their N-terminal cytoplasmic region that would lead to a 3 kDa and 27 kDa form respectively. These forms would however not contain the helix-loop-helix DNA binding domain and thus be inactive. SREBPs in addition contain numerous aspartic acid residues at the amino side of the first transmembrane region, which could be unconventional caspase-cleavage sites. We first compared the migration patterns of the nuclear forms of SREBP-2 obtained through aerolysin activation of caspase-1 or by sterol deprivation. The migration pattern of SREBP-2 was indistinguishable for cells treated with aerolysin or the cholesterol-extracting drug β-methyl cyclodextrin (Figure 3C, 4%–12% acrylamide gradient gels were used to maximize the resolution in the 50 kDa size range), suggesting that cleavage occurred at the same sites and thus possibly by the same enzymes.

To test whether aerolysin-induced activation of SREBP-2 occurs via the well-established SCAP-, S1P-, and S2P-dependent pathway (Goldstein et al., 2006), we performed RNAi against these three proteins (Figure S8). Knocking down the escort protein SCAP or one of the two proteases prevented the aerolysin-induced activation of SREBP-2 (Figure 3D). To further strengthen the involvement of S1P and S2P, we made use of mutant CHO cell lines deficient in either of the proteases (Rawson et al., 1997, 1998). The mature form of SREBP-2 could not be detected in nuclear extracts of aerolysin-treated $S1P^{-/-}$ or $S2P^{-/-}$ cells, in contrast to the recomplemented cells (Figure 3E). SREBP-2 remained full-length in $S1P^{-/-}$ cells, whereas an intermediate, membrane bound form could be detected in $S2P^{-/-}$ cells consistent with a first cleavage event by S1P. Recomplementation of cells with the appropriate protease led to the recovery of toxin-induced SREBP-2 activation. Altogether these observations show that SREBP-2 activation induced by aerolysin depends on SCAP and the sequential processing by S1P and S2P.

Toxin-Induced Activation of the SREBP Pathway Promotes Cell Survival

Having outlined a new signaling pathway linking toxin-induced membrane permeabilization to the activation of lipogenic genes, we investigated whether this pathway plays a role in cell survival. For this, we interfered with different steps along the pathway and monitored cell death by propidium iodide staining. Aerolysin-induced K^+ efflux was prevented by incubating cells in high-K^+ medium. Caspase-1 activation was prevented either by using a caspase-1 inhibitor or RNAi against various components of the inflammasomes, including caspase-1 itself. SREPB2 activation was inhibited using 25-hydroxycholesterol (25OH Chol), a well-established inhibitor of SREBP activation (Wang et al., 1994), by overexpression of INSIG-1 (Castoreno et al., 2005; Yang et al., 2002), a multispanning membrane protein involved in the retention of SREBP-2 in the ER (Goldstein et al., 2006), by RNAi against SCAP, S1P, S2P, or directly against SREBP-1 or -2. And finally, the effect of inhibiting enzymes upregulated by SREBPs was probed by using cerulenin, an inhibitor of fatty acid synthase (Walev et al., 1994).

Death was increased when cells were treated with aerolysin in a high-K^+ medium (Figure 4A). Cell death was also promoted upon simultaneous RNAi knock down of the NALP3 and IPAF inflammasomes (Figure 4B), whereas RNAi against irrelevant proteins had no effect (Figure S6B). Knocking down one of the two inflammasomes, however,

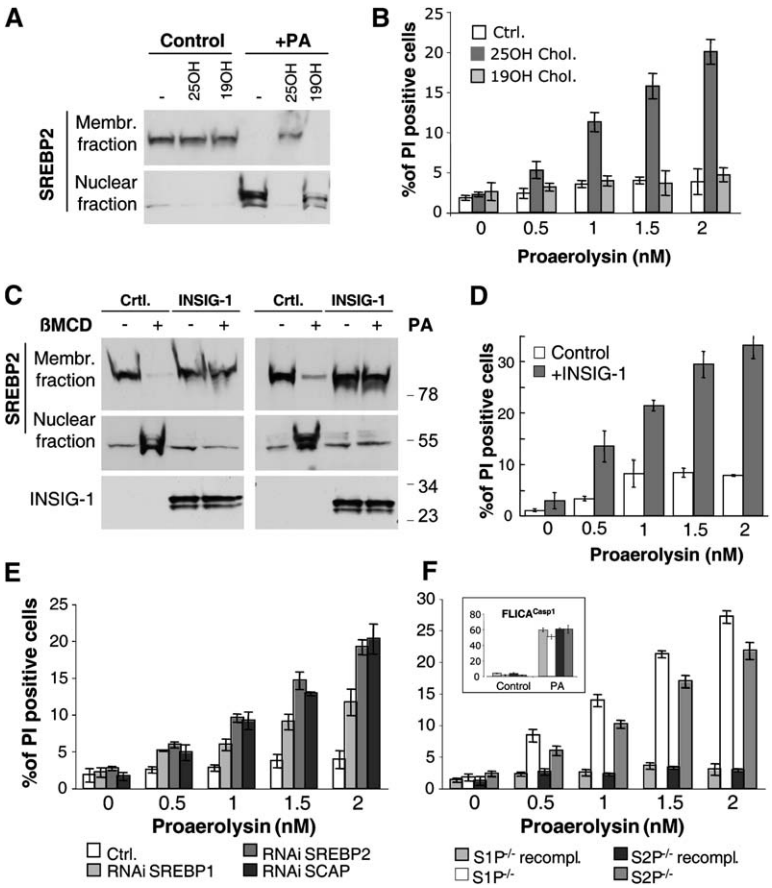

Figure 5. Interfering with the SREBP Pathway Promotes Aerolysin-Induced Cell Death

(A and B) CHO cells were treated or not with 1μg /ml 25 hydroxycholesterol (25OH Chol) or 19 hydroxycholesterol (19OH Chol) for 1 hr at 37°C. In (A), cells were additionally treated or not with 0.2 nM proaerolysin for 3 hr in the presence or not of the drugs. Membrane and nuclear fractions were probed for the presence of SREBP-2. In (B), cells were treated for 1 min with different concentrations of proaerolysin and then incubated in tissue-culture medium, in the presence of the drugs, for 4 hr prior to propidium iodide staining. Error bars represent standard deviations (n = 3).

(C) HeLa cells overexpressing or not human INSIG-1 were treated or not with β methylcyclodextrin (ßMCD, 10 mM) (left panel) or 0.2 nM proaerolysin for 3 hr (right panel). Membrane and nuclear fractions were probed for the presence of SREBP-2. Total cells extracts were probed for myc-tagged INSIG-1.

(D) HeLa cells overexpressing INSIG-1 were treated for 1 min with different concentrations of proaerolysin and then incubated in tissue-culture medium for 4 hr and analyzed as in (B).

(E) HeLa cells were transiently transfected (48 hr) with RNAi duplexes against SREBP-1, SREBP-2, and SCAP. Cells were treated and analyzed as in (B).

(F) S1P- or S2P-deficient CHO cells and the corresponding recomplemented CHO were treated and analyzed as in (B). The inset shows S1P- or S2-deficient CHO cells and corresponding recomplemented cells treated for 3 hr with 0.2 nM proaerolysin. Caspase-1 activation was monitored using $FLICA^{Casp1}$. Error bars represent standard deviations (n = 3).

had no effect on cell death, conditions under which aerolysin-induced caspase-1 activation was only moderately reduced (Figure 2G). In agreement with the death-promoting activity of the inhibitory RNAis, inhibition of caspase-1 using YVAD also led to an increase in cell death, whereas inhibition of caspase-3 had no effect (Figure 4C).

We next inhibited aerolysin-induced activation of SREBP-2 using 25OH Chol (Figure 5A). This drug had no effect on the upstream events such as pore formation (Figure S9A) or caspase-1 activation (Figure S9B). Cell death was however strongly increased (Figure 5B). This effect was specific to aerolysin-induced cell death since 25OH Chol did not enhance death induced by the proapoptotic kinase inhibitor staurosporine (Figure S9C). Increased cell death was not due to the accumulation of toxic insults since 19OH Chol, which does not inhibit SREBP-2 activation (Figure 5B, (Goldstein et al., 2006), as well as two unrelated inhibitors of cellular activities, leupeptin, which inhibits lysosomal enzymes, and bafilomycin, which inhibits the vacuolar proton ATPase, had no effect on aerolysin-induced cell death (Figures 5B and S9D).

As an alternative to 25OH Chol, we overexpressed INSIG-1, which prevented SREBP-2 activation both by sterol extraction with ßMCD (Figure 5C, left panel; Goldstein et al., 2006) and by aerolysin (Figure 5C, right panel). INSIG-1 overexpression had no effect on aerolysin-induced activation of caspase-1 (Figure S9B) but promoted toxin-induced cell death (Figure 5D). Overexpression of two irrelevant proteins, the transmembrane influenza hemaglutinin or the green fluorescent protein, in the same expression vector, had no effect (Figure S10). Finally, we investigated whether inhibiting an enzyme that is upregulated by SREBPs would influence cell death. Cerulenin, an inhibitor of fatty acid synthase (Walev et al., 1994), drastically enhanced aerolysin-induced cell death (Figure S11).

Together these experiments show that interfering with SREBP activation and function promotes cell death in response to aerolysin.

Aeromonas-Triggered Caspase-1-Mediated SREBP-2 Activation Promotes Cell Survival

To test whether the here identified caspase-1-dependent SREBP-2 activation pathway operates during infection by a β-hemolytic bacterium, primary human fibroblasts were infected with *Aeromonas trota*, an aerolysin-producing

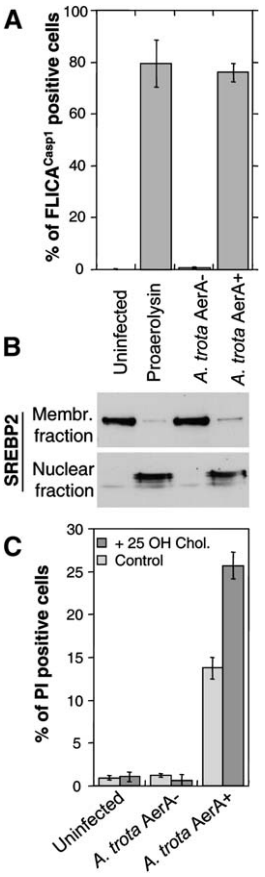

Figure 6. *Aeromonas trota* Triggers Caspase-1-Mediated SREBP-2 Activation in Primary Human Fibroblasts

Primary human fibroblasts were infected with WT ($AerA^+$) or aerolysin-deficient ($AerA^-$) *Aeromonas trota* at an MOI of 1.5 or treated with 0.2 nM proaerolysin.

(A) Caspase-1 activation was monitored using $FLICA^{Casp1}$. Error bars represent standard deviations (n = 3).

(B) Cells were harvested after 3 hr. Membrane and nuclear fractions were probed for the presence of SREBP-2.

(C) Cells were treated or not with 1μg/ml 25 hydroxycholesterol (25OH Chol) for 1 hr at 37°C and then infected as in (A). After 3 hr, cells were stained with propidium iodide. Error bars represent standard deviations (n = 3).

species responsible for severe diarrhea in humans (Chakraborty et al., 1987). The bacterium triggered massive activation of caspase-1, in a strictly aerolysin-dependent manner as demonstrated using the same *Aeromonas* strain in which the aerolysin gene had been selectively inactivated (Figure 6A). Infection of these primary cells with the WT *Aeromonas trota* strain also led to a strong activation of SREBP-2, whereas the aerolysin-deficient strain had no effect (Figure 6B). Finally, WT *Aeromonas*, but not the aerolysin deficient strain, induced cell death, and death was increased in 25OH Chol-treated cells (Figure 6C). Altogether these observations indicate that during infection, aerolysin leads to the activation of caspase-1 and SREBP-2, and this pathway promoted cell survival.

Concluding Remarks

Here we uncovered a novel signaling pathway that links changes in cytoplasmic ion composition, due to plasma membrane permeabilization, to lipid metabolism and cell survival. Although many details remain to be elucidated, our data indicate that, in response to a drop in cytosolic $[K^+]$, the following sequence of events is triggered (Figure 7). The drop in intracellular $[K^+]$ activates the IPAF and ASC/NALP3 inflammasomes and allows the processing of caspase-1. Whether the LRR domains of IPAF and NALP3 are the direct sensors of the $[K^+]$ decrease remains to be shown. Once activated, caspase-1 acts on an intermediate target, which then induces the processing of SREBPs by S1P and S2P. Mature SREBPs then lead to the upregulation of lipogenic genes (Goldstein et al., 2006), which in turn promoted cell survival in response to pore formation.

The present work highlights that caspase-1 may have a far broader role than until now appreciated. In addition to its well-established roles in the production of proinflammatory cytokines (Fantuzzi and Dinarello, 1999) and in mediating cell death upon infection by certain pathogens (for review see Cookson and Brennan, 2001), caspase-1 may be equally important in promoting survival upon pathogen attack as well as having a more general role as a positive regulator of lipid metabolism. To fulfill these additional roles, caspase-1 must modify target proteins other than the precursor forms of interleukins 1β, 18, and 33. The identification of these targets will clearly be of an important future challenge.

Interestingly, whereas we show that a caspase can be an upstream activator of SREBPs, caspases were also found downstream. The gene encoding for caspase-2 was indeed found to be a target of both SREBP-2 (Logette et al., 2005a) and SREBP-1c (Logette et al., 2005b). These findings and the present study suggest a complex interplay between caspases and SREBPs, as well as between intracellular ion composition and lipid metabolism. These mechanisms are likely to be important to regulate lipid homeostasis in mammalian cells, both under physiological conditions and during disease.

Finally, the present study, combined with recent findings in the literature, illustrates the complexity of the cellular response to pore formation by bacterial toxins. Major changes induced by membrane permeabilization include loss of transmembrane potential (Abrami et al., 1998), massive entry of calcium (Krause et al., 1998; Ribardo et al., 2002), osmotic stress (Ratner et al., 2006), and efflux and influx of small ions along their respective gradients (Abrami et al., 1998; Walev et al., 1995). Each of these events appears to trigger signaling pathways, some of which are aimed at warning the immune system, while others appear to promote death or survival of the attacked cell. For example, toxin-induced increases in cytosolic calcium can trigger activation of the NF-κB pathway (Fickl et al., 2005; Ribardo et al., 2002), whereas toxin-induced osmotic stress was found to activate p38 MAPK (Ratner et al., 2006). Interestingly, activation of p38 leads, on one hand, to the release of chemokines such as IL-8 (Ratner

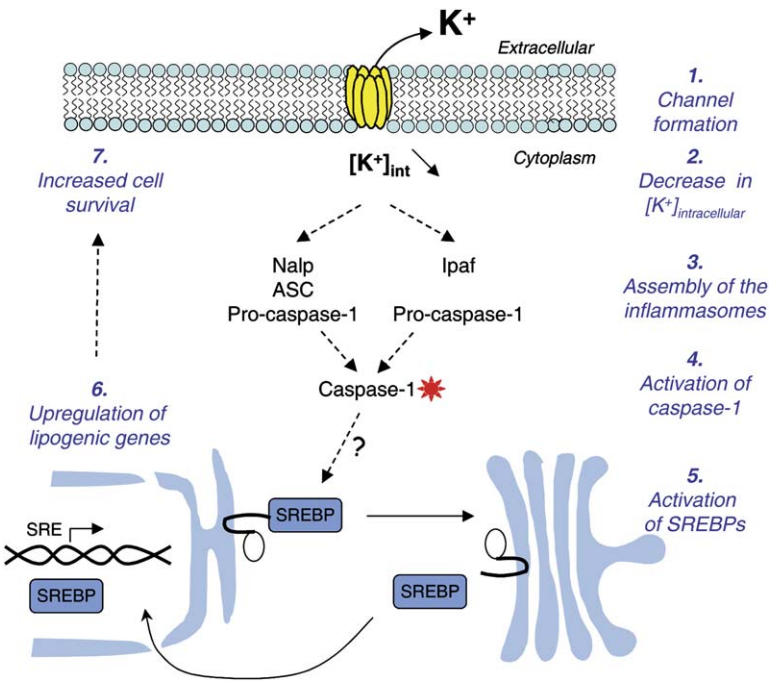

Figure 7. Toxin-Induced Changes in Cytoplasmic Ion Composition Trigger Caspase-1-Dependent SREBP Activation and Cell Survival

Aerolysin leads to the permeabilization of the plasma membrane to ions. Decrease in intracellular potassium triggers the assembly of both IPAF and NALP3 inflammasomes, which allow the activation of caspase-1. Through a yet-to-be-determined intermediate, caspase-1 triggers export of SREBPs from the ER and its subsequent proteolytic processing in the Golgi by S1P and S2P proteases. The released transcription factor migrates to the nucleus, where it activates genes harboring an SRE in their promoter. Lipid metabolic pathways are thus activated. This sequence of events contributes to cell survival.

et al., 2006) and, on the other, switches on a survival pathway, at least in nonimmune cells (Huffman et al., 2004). It indeed appears that, depending on the cell type, survival pathways may be preferentially triggered, whereas in others, in particular cells of the immune system, apoptotic pathways are rapidly switched on (Bantel et al., 2001; Galindo et al., 2004b; Nelson et al., 1999). It will be of interest in the future to identify the full range of cellular changes that are sensed by pore-forming toxin-treated cells, how the cells respond to them, and how the balance between survival and death pathways is regulated.

EXPERIMENTAL PROCEDURES

Cells, Reagents, Cholesterol, and Potassium Determinations

CHO and HeLa cells were grown as described (Abrami et al., 2003). Human fibroblasts were grown in a 15% FCS DMEM medium. SRD-12B cells ($S1P^{-/-}$, [Rawson et al., 1998]) and M19 cells ($S2P^{-/-}$, [Rawson et al., 1997]) deficient in the site 1 and site 2 proteases, respectively, were obtained from J. Goldstein. WT and mutant aerolysins and Staphylococcus α-toxin were purified as described respectively (Buckley, 1990; Vecsey-Semjen et al., 1996). Cerulenin, valinomycin, and 25OH Chol were purchased from Sigma, 19-hydroxycholesterol from Steraloids, Ac-YVAD-chloromethylketone from Bachem, anti-hamster SREBP-2 monoclonal antibodies form ATCC (Clones CRL-2198, Rockville, MD), anti-human SREBP-1 from Santa Cruz, CA, HRP secondary antibodies from Pierce.

Cellular [K^+] was determined by flame photometry using a Philips PYE UNICAM SP9 spectrophotometer (Abrami et al., 1998). Cellular cholesterol was measured using the Ampex Red detection kit (Molecular Probes).

Toxin Treatment, Cell Viability, Subcellular Fractionation, and Biochemical Analyses

Unless specified otherwise, cells were treated with 0.2 nM proaerolysin in tissue-culture medium in the CO_2 incubator. Low-potassium medium refers to Hanks buffer (140 mM NaCl, 5 mM KCl, 10 mM Hepes, 1.3 mM $CaCl_2$, 0.5 mM $MgCl_2$, 0.36 mM K_2HPO_4, 0.44 mM KH_2PO_4, 5.5 mM D-glucose, 4.2 mM $NaHCO_3$), and high-potassium medium was identical with the exception of the NaCl (5 mM) and KCl concentrations (140 mM). Membrane and nuclear extracts were prepared as described (Wang et al., 1994). Eighty micrograms of each fraction was analyzed by SDS-PAGE, followed by Western blotting using an anti-SREBP-2 monoclonal antibody, unless specified otherwise.

Cell Viability and FLICA Staining

Propidium iodide staining (2 μg /ml, Molecular Probes) was performed for 5 min in the CO_2 incubator. Cells are then analyzed by fluorescence-activated cell sorter (FACS). $FLICA^{Casp1}$ (Immunochemistry Technologies), which labels active caspase-1, was added to the culture medium during the last hour of toxin incubation. Cells were then washed, and the number of $FLICA^{Casp1}$-positive cells determined by FACS analysis.

RNA Differential Display

CHO cells were treated or not with 0.1 nM proaerolysin for 1 or 3 hr. RNA differential display was performed according to the described ADDER method (Kornmann et al., 2001). Upregulated messenger bands were extracted from the sequencing gels and processed for sequencing as described (Kornmann et al., 2001).

Immunofluorescence

CHO cells were fixed 15 min with paraformaldehyde 3%, permeabilized with saponin 0.1% in PBS-BSA 0.5% for 5 min, and labeled with anti-SREBP-2 monoclonal antibodies followed by FITC-conjugated secondary antibodies (Molecular Probes). Images were acquired using a 100× lens on an Axiophot (Carl Zeiss Microimaging, Inc.), equipped with a Hamamastu cooled camera using the Openlab acquisition software.

Plasmids, RNAi Duplexes, Transfections, and Real-Time PCR

The *CMV-INSIG-1-Myc* plasmid was from ATCC (Clone 88099). Human ASC was cloned into the *PCR3.V66-Met-FLAG* mammalian

expression vector, human IPAF in the *pCR3.V62-Met-FLAG* vector, human FLAG-NALP3 in the pCR3 vector, and caspase-1 in the pCDNA3 vector. HeLa cells were transfected with 1 μg cDNA/9.6 cm^2 plate using Fugene (Roche Diagnostics Corporation). For gene silencing, HeLa cells were transfected for 24 hr with 200 pmol/9.2 cm^2 dish of siRNA using Oligofectamine (Invitrogen) transfection reagent. The following RNAi duplexes were purchased from Quiagen: AACTG GACCTGCAAGGACTTG against ASC (Dowds et al., 2004), AAGCTT CAGGTGTTGGAATTA and GCATGATCTCTCAGCAAAT against NALP3 and AACTGGGCTCCTCTGTAAATA, and AAGTGCTCTGGAC TTCATTAA against IPAF. siRNAs against S1P from Quiagen, against caspase-1, caspase-3, SCAP, S2P, SREBP-1, and SREBP-2 from Santa Cruz, CA.

For real-time PCR, RNA was extracted from a confluent 10 cm dish of HeLa cells treated or not with proaerolysin and transfected or not with siRNAs using commercial RNA easy miniextraction kits (Quiagen). RNA was quantified by spectrometry and 1 μg was used for reverse transcription using hexanucleotides (Roche). A 1/40 dilution of the cDNA was used to perform the real-time PCR using the Cyber Green reagent (Roche).

Supplemental Data

Supplemental Data include 11 figures and can be found with this article online at http://www.cell.com/cgi/content/full/126/6/1135/DC1/.

ACKNOWLEDGMENTS

We are grateful to C. Lucain for performing the ADDER analysis; S. Thurnheer for technical assistance; A. Dorr for antibody purification; V. Ossipov help with the ADDER analysis; D. Garcin for performing the Sendaï virus infection experiments; and J. Gruenberg, M. Moayeri, and members of the van der Goot lab for critical reading of the manuscript. We thank T. Chakraborty for the *Aeromonas* strains, J. Goldstein for the SDR-12B and M12 mutant cell lines, and S. Clarkson for primary human fibroblasts. We thank the Genomics Platform of the NCCR program "Frontiers in Genetics" for real-time PCR experiments. This work was supported the Swiss National Science Foundation. G. v.d.G. is an international scholar of the Howard Hughes Medical Institute.

Received: January 19, 2006
Revised: April 12, 2006
Accepted: July 24, 2006
Published: September 21, 2006

REFERENCES

Abrami, L., Fivaz, M., Glauser, P.-E., Parton, R.G., and van der Goot, F.G. (1998). A pore-forming toxin interact with a GPI-anchored protein and causes vacuolation of the endoplasmic reticulum. J. Cell Biol. *140*, 525–540.

Abrami, L., Fivaz, M., and van Der Goot, F.G. (2000). Adventures of a pore-forming toxin at the target cell surface. Trends Microbiol. *8*, 168–172.

Abrami, L., Liu, S., Cosson, P., Leppla, S.H., and van der Goot, F.G. (2003). Anthrax toxin triggers endocytosis of its receptor via a lipid raft-mediated clathrin-dependent process. J. Cell Biol. *160*, 321–328.

Abrami, L., and van der Goot, F.G. (1999). Plasma membrane microdomains act as concentration platforms to facilitate intoxication by aerolysin. J. Cell Biol. *147*, 175–184.

Bantel, H., Sinha, B., Domschke, W., Peters, G., Schulze-Osthoff, K., and Janicke, R.U. (2001). alpha-Toxin is a mediator of Staphylococcus aureus-induced cell death and activates caspases via the intrinsic death pathway independently of death receptor signaling. J. Cell Biol. *155*, 637–648.

Bhakdi, S., and Tranum-Jensen, J. (1991). Alpha-toxin of *Staphylococcus aureus*. Microbiol. Rev. *55*, 733–751.

Buckley, J.T. (1990). Purification of cloned proaerolysin released by a low protease mutant of *Aeromonas salmonicida*. Biochem. Cell Biol. *68*, 221–224.

Castoreno, A.B., Wang, Y., Stockinger, W., Jarzylo, L.A., Du, H., Pagnon, J.C., Shieh, E.C., and Nohturfft, A. (2005). Transcriptional regulation of phagocytosis-induced membrane biogenesis by sterol regulatory element binding proteins. Proc. Natl. Acad. Sci. USA *102*, 13129–13134.

Chakraborty, T., Huhle, B., Berghauer, H., and Goebel, W. (1987). Marker exchange mutagenesis of the aerolysin determinant in *Aeromonas hydrophila* demonstrates the role of aerolysin in *A. hydrophila*-associated infections. Infect. Immun. *55*, 2274–2280.

Chamaillard, M., Girardin, S.E., Viala, J., and Philpott, D.J. (2003). Nods, Nalps and Naip: intracellular regulators of bacterial-induced inflammation. Cell. Microbiol. *5*, 581–592.

Chopra, A.K., Xu, X., Ribardo, D., Gonzalez, M., Kuhl, K., Peterson, J.W., and Houston, C.W. (2000). The cytotoxic enterotoxin of Aeromonas hydrophila induces proinflammatory cytokine production and activates arachidonic acid metabolism in macrophages. Infect. Immun. *68*, 2808–2818.

Cookson, B.T., and Brennan, M.A. (2001). Pro-inflammatory programmed cell death. Trends Microbiol. *9*, 113–114.

Demoulin, J.B., Ericsson, J., Kallin, A., Rorsman, C., Ronnstrand, L., and Heldin, C.H. (2004). Platelet-derived growth factor stimulates membrane lipid synthesis through activation of phosphatidylinositol 3-kinase and sterol regulatory element-binding proteins. J. Biol. Chem. *279*, 35392–35402.

Dowds, T.A., Masumoto, J., Zhu, L., Inohara, N., and Nunez, G. (2004). Cryopyrin-induced interleukin 1beta secretion in monocytic cells: enhanced activity of disease-associated mutants and requirement for ASC. J. Biol. Chem. *279*, 21924–21928.

Fantuzzi, G., and Dinarello, C.A. (1999). Interleukin-18 and interleukin-1 beta: two cytokine substrates for ICE (caspase-1). J. Clin. Immunol. *19*, 1–11.

Fickl, H., Cockeran, R., Steel, H.C., Feldman, C., Cowan, G., Mitchell, T.J., and Anderson, R. (2005). Pneumolysin-mediated activation of NFkappaB in human neutrophils is antagonized by docosahexaenoic acid. Clin. Exp. Immunol. *140*, 274–281.

Fivaz, M., Vilbois, F., Thurnheer, S., Pasquali, C., Abrami, L., Bickel, P., Parton, R., and van der Goot, F. (2002). Differential sorting and fate of endocytosed GPI-anchored proteins. EMBO J. *21*, 3989–4000.

Franchi, L., Amer, A., Body-Malapel, M., Kanneganti, T.D., Ozoren, N., Jagirdar, R., Inohara, N., Vandenabeele, P., Bertin, J., Coyle, A., et al. (2006). Cytosolic flagellin requires Ipaf for activation of caspase-1 and interleukin 1beta in salmonella-infected macrophages. Nat. Immunol. *7*, 576–582.

Galindo, C.L., Fadl, A.A., Sha, J., and Chopra, A.K. (2004a). Microarray analysis of Aeromonas hydrophila cytotoxic enterotoxin-treated murine primary macrophages. Infect. Immun. *72*, 5439–5445.

Galindo, C.L., Fadl, A.A., Sha, J., Gutierrez, C., Jr., Popov, V.L., Boldogh, I., Aggarwal, B.B., and Chopra, A.K. (2004b). Aeromonas hydrophila cytotoxic enterotoxin activates mitogen-activated protein kinases and induces apoptosis in murine macrophages and human intestinal epithelial cells. J. Biol. Chem. *279*, 37597–37612.

Goldstein, J.L., DeBose-Boyd, R.A., and Brown, M.S. (2006). Protein sensors for membrane sterols. Cell *124*, 35–46.

Horton, J.D., and Shimomura, I. (1999). Sterol regulatory element-binding proteins: activators of cholesterol and fatty acid biosynthesis. Curr. Opin. Lipidol. *10*, 143–150.

Huffman, D.L., Abrami, L., Sasik, R., Corbeil, J., van der Goot, F.G., and Aroian, R.V. (2004). Mitogen-activated protein kinase pathways defend against bacterial pore-forming toxins. Proc. Natl. Acad. Sci. USA *101*, 10995–11000.

Iacovache, I., Paumard, P., Scheib, H., Lesieur, C., Sakai, N., Matile, S., Parker, M.W., and van der Goot, F.G. (2006). A rivet model for channel formation by aerolysin-like pore-forming toxins. EMBO J. *25*, 456–466.

Kahlenberg, J.M., and Dubyak, G.R. (2004). Mechanisms of caspase-1 activation by P2X7 receptor-mediated K+ release. Am. J. Physiol. Cell Physiol. *286*, C1100–C1108.

Kanneganti, D.-T., Özören, N., Body-Malapel, M., Amer, A., Park, J.-H., Franchi, F., Whitfield, J., Barchet, W., Colonna, M., Vandenabeele, P., et al. (2006). Bacterial RNA and small antiviral compounds activate caspase-1 through cryopyrin/Nalp3. Nature *440*, 233–236.

Kornmann, B., Preitner, N., Rifat, D., Fleury-Olela, F., and Schibler, U. (2001). Analysis of circadian liver gene expression by ADDER, a highly sensitive method for the display of differentially expressed mRNAs. Nucleic Acids Res. *29*, E51.

Krause, K.H., Fivaz, M., Monod, A., and van der Goot, F.G. (1998). Aerolysin induces G-protein activation and Ca2+ release from intracellular stores in human granulocytes. J. Biol. Chem. *273*, 18122–18129.

Lee, J.N., and Ye, J. (2004). Proteolytic activation of sterol regulatory element-binding protein induced by cellular stress through depletion of Insig-1. J. Biol. Chem. *279*, 45257–45265.

Logette, E., Le Jossic-Corcos, C., Masson, D., Solier, S., Sequeira-Legrand, A., Dugail, I., Lemaire-Ewing, S., Desoche, L., Solary, E., and Corcos, L. (2005a). Caspase-2, a novel lipid sensor under the control of sterol regulatory element binding protein 2. Mol. Cell. Biol. *25*, 9621–9631.

Logette, E., Solary, E., and Corcos, L. (2005b). Identification of a functional DNA binding site for the SREBP-1c transcription factor in the first intron of the human caspase-2 gene. Biochim. Biophys. Acta. *1738*, 1–5.

Mariathasan, S., Newton, K., Monack, D.M., Vucic, D., French, D.M., Lee, W.P., Roose-Girma, M., Erickson, S., and Dixit, V.M. (2004). Differential activation of the inflammasome by caspase-1 adaptors ASC and Ipaf. Nature *430*, 213–218.

Mariathasan, S., Weiss, D.S., Newton, N., McBride, J., O'Rourke, K., Roose-Girma, R., Lee, W., Weinrauch, Y., Monack, D.M., and Dixit, V.M. (2006). Cryopyrin activates the inflammasome in response to toxins and ATP. Nature *440*, 228–232.

Martinon, F., Pétrilli, V., Mayor, A., Tardivel, A., and Tschopp, J. (2006). Gout-associated uric acid crystals activate the NALP3 inflammasome. Nature *440*, 237–241.

Martinon, F., and Tschopp, J. (2005). NLRs join TLRs as innate sensors of pathogens. Trends Immunol. *26*, 447–454.

Miao, E.A., Alpuche-Aranda, C.M., Dors, M., Clark, A.E., Bader, M.W., Miller, S.I., and Aderem, A. (2006). Cytoplasmic flagellin activates caspase-1 and secretion of interleukin 1beta via Ipaf. Nat. Immunol. *7*, 569–575.

Mota, L.J., Sorg, I., and Cornelis, G.R. (2005). Type III secretion: the bacteria-eukaryotic cell express. FEMS Microbiol. Lett. *252*, 1–10.

Nadeau, K.J., Leitner, J.W., Gurerich, I., and Draznin, B. (2004). Insulin regulation of sterol regulatory element-binding protein-1 expression in L-6 muscle cells and 3T3 L1 adipocytes. J. Biol. Chem. *279*, 34380–34387.

Nelson, K.L., Brodsky, R.A., and Buckley, J.T. (1999). Channels formed by subnanomalar concentrations of the toxin aerolysin trigger apoptosis of T lymphomas. Cell. Microbiol. *1*, 69–74.

Perregaux, D., and Gabel, C.A. (1994). Interleukin-1 beta maturation and release in response to ATP and nigericin. Evidence that potassium depletion mediated by these agents is a necessary and common feature of their activity. J. Biol. Chem. *269*, 15195–15203.

Ratner, A.J., Hippe, K.R., Aguilar, J.L., Bender, M.H., Nelson, A.L., and Weiser, J.N. (2006). Epithelial cells are sensitive detectors of bacterial pore-forming toxins. J Biol. Chem. *281*, 12994–12998.

Rawson, R.B., Cheng, D., Brown, M.S., and Goldstein, J.L. (1998). Isolation of cholesterol-requiring mutant Chinese hamster ovary cells with defects in cleavage of sterol regulatory element-binding proteins at site 1. J. Biol. Chem. *273*, 28261–28269.

Rawson, R.B., Zelenski, N.G., Nijhawan, D., Ye, J., Sakai, J., Hasan, M.T., Chang, T.Y., Brown, M.S., and Goldstein, J.L. (1997). Complementation cloning of S2P, a gene encoding a putative metalloprotease required for intramembrane cleavage of SREBPs. Mol. Cell *1*, 47–57.

Ribardo, D.A., Kuhl, K.R., Boldogh, I., Peterson, J.W., Houston, C.W., and Chopra, A.K. (2002). Early cell signaling by the cytotoxic enterotoxin of Aeromonas hydrophila in macrophages. Microb. Pathog. *32*, 149–163.

Schmitz, J., Owyang, A., Oldham, E., Song, Y., Murphy, E., McClanahan, T.K., Zurawski, G., Moshrefi, M., Qin, J., Li, X., et al. (2005). IL-33, an interleukin-1-like cytokine that signals via the il-1 receptor-related protein st 2 and induces t helper type 2-associated cytokines. Immunity *23*, 479–490.

Shatursky, O., Heuck, A.P., Shepard, L.A., Rossjohn, J., Parker, M.W., Johnson, A.E., and Tweten, R.K. (1999). The mechanism of membrane insertion for a cholesterol-dependent cytolysin: a novel paradigm for pore-forming toxins. Cell *99*, 293–299.

Strahle, L., Garcin, D., and Kolakofsky, D. (2006). Sendai virus defective-interfering genomes and the activation of interferon-beta. Virology *351*, 101–111.

Sutterwala, F.S., Ogura, Y., Szczepanik, M., Lara-Tejero, M., Lichtenberger, G.S., Grant, E.P., Bertin, J., Coyle, A.J., Galan, J.E., Askenase, P.W., and Flavell, R.A. (2006). Critical role for NALP3/CIAS1/cryopyrin in innate and adaptive immunity through its regulation of caspase-1. Immunity *24*, 317–327.

Tsitrin, Y., Morton, C.J., El Bez, C., Paumard, P., Velluz, M.C., Adrian, M., Dubochet, J., Parker, M.W., Lanzavecchia, S., and Van Der Goot, F.G. (2002). Conversion of a transmembrane to a water-soluble protein complex by a single point mutation. Nat. Struct. Biol. *9*, 729–733.

F.G. van der Goot, ed. (2001). Pore-forming toxins (Heidelberg, Germany: Springer-Verlag).

Vecsey-Semjen, B., Mollby, R., and van der Goot, F.G. (1996). Partial C-terminal unfolding is required for channel formation by staphylococcal alpha-toxin. J. Biol. Chem. *271*, 8655–8660.

Walev, I., Bhakdi, S.C., Hofmann, F., Djonder, N., Valeva, A., Aktories, K., and Bhakdi, S. (2001). Delivery of proteins into living cells by reversible membrane permeabilization with streptolysin-O. Proc. Natl. Acad. Sci. USA *98*, 3185–3190.

Walev, I., Klein, J., Husmann, M., Valeva, A., Strauch, S., Wirtz, H., Weichel, O., and Bhakdi, S. (2000). Potassium regulates IL-1 beta processing via calcium-independent phospholipase A2. J. Immunol. *164*, 5120–5124.

Walev, I., Palmer, M., Martin, E., Jonas, D., Weller, U., Hohn, B.H., Husmann, M., and Bhakdi, S. (1994). Recovery of human fibroblasts from attack by the pore-forming alpha- toxin of Staphylococcus aureus. Microb. Pathog. *17*, 187–201.

Walev, I., Reske, K., Palmer, M., Valeva, A., and Bhakdi, S. (1995). Potassium-inhibited processing of IL-1 beta in human monocytes. EMBO J. *14*, 1607–1614.

Wang, X., Sato, R., Brown, M.S., Hua, X., and Goldstein, J.L. (1994). SREBP-1, a membrane-bound transcription factor released by sterol-regulated proteolysis. Cell *77*, 53–62.

Yang, T., Espenshade, P.J., Wright, M.E., Yabe, D., Gong, Y., Aebersold, R., Goldstein, J.L., and Brown, M.S. (2002). Crucial step in cholesterol homeostasis: sterols promote binding of SCAP to INSIG-1, a membrane protein that facilitates retention of SREBPs in ER. Cell *110*, 489–500.